Search for the radiative penguin decays $B^0 \to K_S^0 K_S^0 \gamma$ in the Belle experiment

H. B. Jeon,[47,*] K. H. Kang,[42] H. Park,[47] I. Adachi,[21,17] H. Aihara,[90] S. Al Said,[83,43] D. M. Asner,[3] H. Atmacan,[8] T. Aushev,[23] R. Ayad,[83] V. Babu,[9] S. Bahinipati,[27] P. Behera,[30] K. Belous,[34] J. Bennett,[57] F. Bernlochner,[2] M. Bessner,[20] V. Bhardwaj,[26] B. Bhuyan,[28] T. Bilka,[5] A. Bobrov,[4,69] D. Bodrov,[23,48] J. Borah,[28] A. Bozek,[66] M. Bračko,[54,40] P. Branchini,[36] T. E. Browder,[20] A. Budano,[36] M. Campajola,[35,61] D. Červenkov,[5] M.-C. Chang,[13] P. Chang,[65] A. Chen,[63] B. G. Cheon,[19] K. Chilikin,[48] H. E. Cho,[19] K. Cho,[45] S.-J. Cho,[96] S.-K. Choi,[7] Y. Choi,[81] S. Choudhury,[38] D. Cinabro,[94] S. Cunliffe,[9] S. Das,[53] N. Dash,[30] G. De Pietro,[36] R. Dhamija,[29] F. Di Capua,[35,61] J. Dingfelder,[2] Z. Doležal,[5] T. V. Dong,[11] D. Epifanov,[4,69] T. Ferber,[9] D. Ferlewicz,[56] B. G. Fulsom,[72] R. Garg,[73] V. Gaur,[93] N. Gabyshev,[4,69] A. Giri,[29] P. Goldenzweig,[41] B. Golob,[50,40] E. Graziani,[36] T. Gu,[74] K. Gudkova,[4,69] C. Hadjivasiliou,[72] T. Hara,[21,17] K. Hayasaka,[68] H. Hayashii,[62] M. T. Hedges,[20] T. Higuchi,[42] W.-S. Hou,[65] C.-L. Hsu,[82] K. Inami,[60] G. Inguglia,[33] A. Ishikawa,[21,17] R. Itoh,[21,17] M. Iwasaki,[71] Y. Iwasaki,[21] W. W. Jacobs,[31] E.-J. Jang,[18] S. Jia,[14] Y. Jin,[90] K. K. Joo,[6] J. Kahn,[41] H. Kakuno,[92] A. B. Kaliyar,[84] T. Kawasaki,[44] C. Kiesling,[55] C. H. Kim,[19] D. Y. Kim,[80] K.-H. Kim,[96] K. T. Kim,[46] Y.-K. Kim,[96] K. Kinoshita,[8] P. Kodyš,[5] T. Konno,[44] A. Korobov,[4,69] S. Korpar,[54,40] E. Kovalenko,[4,69] P. Križan,[50,40] R. Kroeger,[57] P. Krokovny,[4,69] T. Kuhr,[51] M. Kumar,[53] K. Kumara,[94] A. Kuzmin,[4,69,48] Y.-J. Kwon,[96] Y.-T. Lai,[42] K. Lalwani,[53] T. Lam,[93] J. S. Lange,[15] M. Laurenza,[36,77] S. C. Lee,[47] C. H. Li,[49] J. Li,[47] Y. Li,[14] Y. B. Li,[14] L. Li Gioi,[55] J. Libby,[30] K. Lieret,[51] D. Liventsev,[94,21] A. Martini,[97] M. Masuda,[89,75] T. Matsuda,[58] D. Matvienko,[4,69,48] S. K. Maurya,[28] M. Merola,[35,61] F. Metzner,[41] K. Miyabayashi,[62] R. Mizuk,[48,23] G. B. Mohanty,[84] M. Nakao,[21,17] D. Narwal,[28] Z. Natkaniec,[66] A. Natochii,[20] L. Nayak,[29] M. Nayak,[86] N. K. Nisar,[3] S. Nishida,[21,17] K. Ogawa,[68] S. Ogawa,[87] H. Ono,[67,68] Y. Onuki,[90] P. Oskin,[48] P. Pakhlov,[48,59] G. Pakhlova,[23,48] T. Pang,[74] S. Pardi,[35] S.-H. Park,[21] A. Passeri,[36] S. Patra,[26] S. Paul,[85,55] T. K. Pedlar,[52] R. Pestotnik,[40] L. E. Piilonen,[93] T. Podobnik,[50,40] V. Popov,[23] E. Prencipe,[24] M. T. Prim,[2] M. V. Purohit,[70] M. Röhrken,[9] A. Rostomyan,[9] N. Rout,[30] G. Russo,[61] D. Sahoo,[38] S. Sandilya,[29] A. Sangal,[8] L. Santelj,[50,40] T. Sanuki,[88] V. Savinov,[74] G. Schnell,[1,25] C. Schwanda,[33] Y. Seino,[68] K. Senyo,[95] M. E. Sevior,[56] M. Shapkin,[34] C. Sharma,[53] V. Shebalin,[20] C. P. Shen,[14] J.-G. Shiu,[65] J. B. Singh,[73,†] A. Sokolov,[34] E. Solovieva,[48] M. Starič,[40] Z. S. Stottler,[93] J. F. Strube,[72] M. Sumihama,[16,75] T. Sumiyoshi,[92] M. Takizawa,[79,22,76] U. Tamponi,[37] K. Tanida,[39] F. Tenchini,[9] M. Uchida,[91] T. Uglov,[48,23] Y. Unno,[19] S. Uno,[21,17] P. Urquijo,[56] Y. Usov,[4,69] S. E. Vahsen,[20] R. Van Tonder,[2] G. Varner,[20] K. E. Varvell,[82] A. Vinokurova,[4,69] A. Vossen,[10] E. Waheed,[21] C. H. Wang,[64] M.-Z. Wang,[65] S. Watanuki,[96] E. Won,[46] B. D. Yabsley,[82] W. Yan,[78] S. B. Yang,[46] H. Ye,[9] J. Yelton,[12] J. H. Yin,[46] C. Z. Yuan,[32] Y. Yusa,[68] Y. Zhai,[38] Z. P. Zhang,[78] V. Zhilich,[4,69] and V. Zhukova[48]

(Belle Collaboration)

[1]*Department of Physics, University of the Basque Country UPV/EHU, 48080 Bilbao*
[2]*University of Bonn, 53115 Bonn*
[3]*Brookhaven National Laboratory, Upton, New York 11973*
[4]*Budker Institute of Nuclear Physics SB RAS, Novosibirsk 630090*
[5]*Faculty of Mathematics and Physics, Charles University, 121 16 Prague*
[6]*Chonnam National University, Gwangju 61186*
[7]*Chung-Ang University, Seoul 06974*
[8]*University of Cincinnati, Cincinnati, Ohio 45221*
[9]*Deutsches Elektronen–Synchrotron, 22607 Hamburg*
[10]*Duke University, Durham, North Carolina 27708*
[11]*Institute of Theoretical and Applied Research (ITAR), Duy Tan University, Hanoi 100000*
[12]*University of Florida, Gainesville, Florida 32611*
[13]*Department of Physics, Fu Jen Catholic University, Taipei 24205*
[14]*Key Laboratory of Nuclear Physics and Ion-beam Application (MOE) and Institute of Modern Physics, Fudan University, Shanghai 200443*
[15]*Justus-Liebig-Universität Gießen, 35392 Gießen*
[16]*Gifu University, Gifu 501-1193*
[17]*SOKENDAI (The Graduate University for Advanced Studies), Hayama 240-0193*
[18]*Gyeongsang National University, Jinju 52828*
[19]*Department of Physics and Institute of Natural Sciences, Hanyang University, Seoul 04763*
[20]*University of Hawaii, Honolulu, Hawaii 96822*
[21]*High Energy Accelerator Research Organization (KEK), Tsukuba 305-0801*

[22]*J-PARC Branch, KEK Theory Center, High Energy Accelerator Research Organization (KEK), Tsukuba 305-0801*
[23]*National Research University Higher School of Economics, Moscow 101000*
[24]*Forschungszentrum Jülich, 52425 Jülich*
[25]*IKERBASQUE, Basque Foundation for Science, 48013 Bilbao*
[26]*Indian Institute of Science Education and Research Mohali, SAS Nagar 140306*
[27]*Indian Institute of Technology Bhubaneswar, Satya Nagar 751007*
[28]*Indian Institute of Technology Guwahati, Assam 781039*
[29]*Indian Institute of Technology Hyderabad, Telangana 502285*
[30]*Indian Institute of Technology Madras, Chennai 600036*
[31]*Indiana University, Bloomington, Indiana 47408*
[32]*Institute of High Energy Physics, Chinese Academy of Sciences, Beijing 100049*
[33]*Institute of High Energy Physics, Vienna 1050*
[34]*Institute for High Energy Physics, Protvino 142281*
[35]*INFN—Sezione di Napoli, I-80126 Napoli*
[36]*INFN—Sezione di Roma Tre, I-00146 Roma*
[37]*INFN—Sezione di Torino, I-10125 Torino*
[38]*Iowa State University, Ames, Iowa 50011*
[39]*Advanced Science Research Center, Japan Atomic Energy Agency, Naka 319-1195*
[40]*J. Stefan Institute, 1000 Ljubljana*
[41]*Institut für Experimentelle Teilchenphysik, Karlsruher Institut für Technologie, 76131 Karlsruhe*
[42]*Kavli Institute for the Physics and Mathematics of the Universe (WPI), University of Tokyo, Kashiwa 277-8583*
[43]*Department of Physics, Faculty of Science, King Abdulaziz University, Jeddah 21589*
[44]*Kitasato University, Sagamihara 252-0373*
[45]*Korea Institute of Science and Technology Information, Daejeon 34141*
[46]*Korea University, Seoul 02841*
[47]*Kyungpook National University, Daegu 41566*
[48]*P.N. Lebedev Physical Institute of the Russian Academy of Sciences, Moscow 119991*
[49]*Liaoning Normal University, Dalian 116029*
[50]*Faculty of Mathematics and Physics, University of Ljubljana, 1000 Ljubljana*
[51]*Ludwig Maximilians University, 80539 Munich*
[52]*Luther College, Decorah, Iowa 52101*
[53]*Malaviya National Institute of Technology Jaipur, Jaipur 302017*
[54]*Faculty of Chemistry and Chemical Engineering, University of Maribor, 2000 Maribor*
[55]*Max-Planck-Institut für Physik, 80805 München*
[56]*School of Physics, University of Melbourne, Victoria 3010*
[57]*University of Mississippi, University, Mississippi 38677*
[58]*University of Miyazaki, Miyazaki 889-2192*
[59]*Moscow Physical Engineering Institute, Moscow 115409*
[60]*Graduate School of Science, Nagoya University, Nagoya 464-8602*
[61]*Università di Napoli Federico II, I-80126 Napoli*
[62]*Nara Women's University, Nara 630-8506*
[63]*National Central University, Chung-li 32054*
[64]*National United University, Miao Li 36003*
[65]*Department of Physics, National Taiwan University, Taipei 10617*
[66]*H. Niewodniczanski Institute of Nuclear Physics, Krakow 31-342*
[67]*Nippon Dental University, Niigata 951-8580*
[68]*Niigata University, Niigata 950-2181*
[69]*Novosibirsk State University, Novosibirsk 630090*
[70]*Okinawa Institute of Science and Technology, Okinawa 904-0495*
[71]*Osaka City University, Osaka 558-8585*
[72]*Pacific Northwest National Laboratory, Richland, Washington 99352*
[73]*Panjab University, Chandigarh 160014*
[74]*University of Pittsburgh, Pittsburgh, Pennsylvania 15260*
[75]*Research Center for Nuclear Physics, Osaka University, Osaka 567-0047*
[76]*Meson Science Laboratory, Cluster for Pioneering Research, RIKEN, Saitama 351-0198*
[77]*Dipartimento di Matematica e Fisica, Università di Roma Tre, I-00146 Roma*
[78]*Department of Modern Physics and State Key Laboratory of Particle Detection and Electronics, University of Science and Technology of China, Hefei 230026*

[79]Showa Pharmaceutical University, Tokyo 194-8543
[80]Soongsil University, Seoul 06978
[81]Sungkyunkwan University, Suwon 16419
[82]School of Physics, University of Sydney, New South Wales 2006
[83]Department of Physics, Faculty of Science, University of Tabuk, Tabuk 71451
[84]Tata Institute of Fundamental Research, Mumbai 400005
[85]Department of Physics, Technische Universität München, 85748 Garching
[86]School of Physics and Astronomy, Tel Aviv University, Tel Aviv 69978
[87]Toho University, Funabashi 274-8510
[88]Department of Physics, Tohoku University, Sendai 980-8578
[89]Earthquake Research Institute, University of Tokyo, Tokyo 113-0032
[90]Department of Physics, University of Tokyo, Tokyo 113-0033
[91]Tokyo Institute of Technology, Tokyo 152-8550
[92]Tokyo Metropolitan University, Tokyo 192-0397
[93]Virginia Polytechnic Institute and State University, Blacksburg, Virginia 24061
[94]Wayne State University, Detroit, Michigan 48202
[95]Yamagata University, Yamagata 990-8560
[96]Yonsei University, Seoul 03722
[97]Deutsches Elektronen-Synchrotron, 22607 Hamburg

(Received 11 March 2022; accepted 12 July 2022; published 25 July 2022)

We report results from the first search for the rare penguin-dominated decay mode $B^0 \to K_S^0 K_S^0 \gamma$, which can result from the production of tensor mesons $f(1270)$ and $f'(1525)$ in association with a photon. The search uses the full data sample of 772×10^6 $B\bar{B}$ pairs collected with the Belle detector at the KEKB asymmetric-energy e^+e^- collider. No statistically significant signals are observed in the $K_S^0 K_S^0$ invariant mass range $1\ \mathrm{GeV}/c^2 < M_{K_S^0 K_S^0} < 3\ \mathrm{GeV}/c^2$, and the following upper limits at the 90% confidence level are obtained: $\mathcal{B}(B^0 \to K_S^0 K_S^0 \gamma) < 5.8 \times 10^{-7}$, $\mathcal{B}(B^0 \to f_2 \gamma) \times \mathcal{B}(f_2(1270) \to K_S^0 K_S^0) < 3.1 \times 10^{-7}$, and $\mathcal{B}(B^0 \to f_2' \gamma) \times \mathcal{B}(f_2'(1525) \to K_S^0 K_S^0) < 2.1 \times 10^{-7}$. In addition, 90% confidence-level upper limits in the range of $[0.7\text{–}2.9] \times 10^{-7}$ are also obtained on the $B^0 \to K_S^0 K_S^0 \gamma$ branching fraction in bins of $M_{K_S^0 K_S^0}$.

DOI: 10.1103/PhysRevD.106.012006

Radiative $b \to s\gamma$ and $b \to d\gamma$ quark transitions are flavor-changing-neutral-current processes and are not allowed at tree level in the Standard Model (SM). Such decays proceed predominantly through radiative loop diagrams, referred to as radiative penguin diagrams [1], and are potentially sensitive to contributions from non-SM particles that can appear in the loop. For example, the two Higgs doublet model (2HDM) introduces an additional doublet of Higgs fields, and the associated charged Higgs boson can appear in the loop instead of the W. Wilson coefficients in the operator product expansion [2] are modified to include the effect of the 2HDM [3] and this new term depends on the mass of the charged Higgs [4]. Thus, assuming that effects from strong interaction corrections can be controlled, a disparity in the measured branching fraction with respect to SM expectations can be interpreted as arising from a new physics contribution.

In the SM, the $b \to d\gamma$ process is suppressed relative to $b \to s\gamma$ by the squared ratio of Cabibbo-Kobayashi-Maskawa matrix elements $|V_{td}/V_{ts}|^2$ [5]. The predicted branching fractions [6] and experimental world averages [7] for $b \to s\gamma$ and $b \to d\gamma$ are in agreement at the 1σ and $\sim 2.5\sigma$ level, respectively. Branching fractions of several exclusive $b \to s\gamma$ modes have been measured: $B \to K^*\gamma$ [8]; $B \to K_1(1270)\gamma$ [9]; $B \to \phi K\gamma$ [10]; $B \to K\eta'\gamma$ [11]; $B \to K\eta\gamma$ [12]. On the other hand, $B \to \rho\gamma$ and $B \to \omega\gamma$ are the only observed exclusive $b \to d\gamma$ modes [13] and measurements of additional exclusive X_d final states are needed.

The $B^0 \to K_S^0 K_S^0 \gamma$ decay, shown in Fig. 1, arises from a $b \to d\gamma$ transition and can proceed via a number of different intermediate states. Because the $K_S^0 K_S^0$ system consists of two identical spinless particles, Bose-Einstein statistics requires that the angular momentum quantum number of this system, in its rest frame, must be even. If the system is produced in the decay of an intermediate-state parent meson, this meson must therefore have even spin. In

[*]Present address: the Enrico Fermi Institute of the University of Chicago, Chicago, Illinois 60637.
[†]Also at University of Petroleum and Energy Studies, Dehradun 248007.

Published by the American Physical Society under the terms of the Creative Commons Attribution 4.0 International license. Further distribution of this work must maintain attribution to the author(s) and the published article's title, journal citation, and DOI. Funded by SCOAP³.

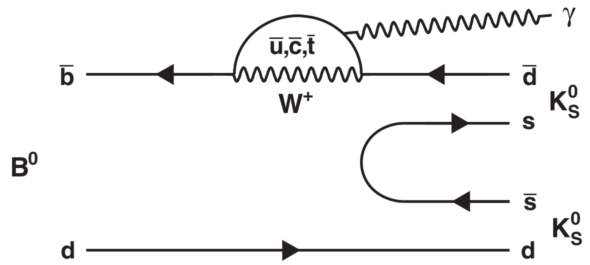

FIG. 1. $b \to d\gamma$ penguin diagram for $B^0 \to K_S^0 K_S^0 \gamma$ decay.

addition, the photon, as a massless $J = 1$ particle, can only have helicities $\lambda = \pm 1$ along the B-meson decay axis. The sum of the spin projections of the particles along this axis must be zero, since $J(B) = 0$ and there cannot be any projection of the orbital angular momentum along this axis. As a consequence, the $K_S^0 K_S^0$ system cannot be a spin-0 system, and its lowest allowed value is $J = 2$. This constraint motivates the search for the $J = 2$ mesons $f_2(1270)$ and $f_2'(1525)$, which can decay into the $K_S^0 K_S^0$ final state. This paper presents results from a search for the $B^0 \to K_S^0 K_S^0 \gamma$ decay, where the $K_S^0 K_S^0$ system is also studied for evidence of an intermediate-state tensor meson.

The $\Upsilon(4S)$ meson is produced at the KEKB asymmetric-energy e^+e^- collider [14] with electrons and positrons having energies of 8 GeV and 3.5 GeV, respectively, and subsequently decays to $B\bar{B}$ pairs which are nearly at rest in the center-of-mass system (CMS). The z axis is defined as opposite to the e^+ beam direction. We search for the decay $B^0 \to K_S^0 K_S^0 \gamma$ using the full data sample of $(772 \pm 11) \times 10^6 B\bar{B}$ pairs collected at the $\Upsilon(4S)$ resonance with the Belle detector at the KEKB asymmetric-energy e^+e^- collider. This is the first search for a B^0 decay to two pseudoscalars K_S^0 with a prompt photon in the final state.

The Belle detector, a hermetic magnetic spectrometer designed to detect the decay products of B mesons, consists of a silicon vertex detector, a 50-layer central drift chamber (CDC), an array of aerogel threshold Cherenkov counters, a barrellike arrangement of time-of-flight scintillation counters, and an electromagnetic calorimeter comprised of CsI(Tl) scintillation crystals (ECL). These detector components, providing high vertex resolution, good tracking, sophisticated particle identification capability, and excellent calorimetry, are located inside a superconducting solenoid coil providing a 1.5 T magnetic field. An iron flux-return is located outside of the magnetic coil which is instrumented to detect K_L^0 mesons and identify muons. The detector is described in detail elsewhere [15].

The event selections are optimized using simulated Monte Carlo (MC) samples. The MC samples for the signal and background processes are generated with E VTG EN [16] and the detector response is then simulated using G EANT3 [17]. Any environmental changes in the Belle detector and KEKB accelerator machine during the operations are reflected in the detector simulation. To generate the signal MC sample of B^0 decaying to a tensor meson (as an intermediate state) and a prompt photon, a two-body decay model is used with equal helicity amplitudes for the allowed tensor-meson helicities of ± 1. The decay of the intermediate state system to $K_S^0 K_S^0$ is then simulated. To allow for study of the $K_S^0 K_S^0 \gamma$ system across the full kinematically accessible range in $m(K_S^0 K_S^0)$, simulated signal events are distributed uniformly in the range $1\ \mathrm{GeV}/c^2 < m(K_S^0 K_S^0) < 3\ \mathrm{GeV}/c^2$.

Photons must have no associated tracks in the CDC, be in the ECL barrel region ($33° < \theta_\gamma < 128°$), and have a 95% or higher fraction of energy deposition in the central 3×3 of 5×5 ECL crystals centered on the highest energy deposit crystal. The center-of-mass energy of the prompt photon candidate, E_γ, must satisfy the requirement $1.6\ \mathrm{GeV} < E_\gamma < 2.8\ \mathrm{GeV}$. Most background photons originate from $\pi^0 \to \gamma\gamma$ and $\eta \to \gamma\gamma$ decays. We combine the photon candidate with all other photons with momenta larger than $50\ \mathrm{MeV}/c$ in the event and calculate the probabilities of the reconstructed photon candidate to be π^0-like or η-like [18]. Backgrounds are suppressed by removing π^0-like and η-like candidates using a likelihood-based selector. About 86% of the photons from the signal B are retained and about 62% from the accompanying B are rejected. If more than one candidate satisfies the selection criteria for the prompt photon, the most energetic photon is chosen as the prompt photon candidate. The selection efficiency of the prompt photon is approximately 50%, and 99.5% are found to be correctly matched in signal MC sample.

K_S^0 candidates are reconstructed from two oppositely charged tracks. A displaced vertex consistent with $K_S^0 \to \pi^+\pi^-$ decay is required using a neural network (NN) discriminator with 20 inputs [19]; this selection also suppresses $\Lambda \to p\pi^-$ decays. The invariant mass of the pion pairs is then required to satisfy $|M_{\pi\pi} - m_{K_S^0}| < 4.7\ \mathrm{MeV}/c^2$, corresponding to a $\pm 2.6\sigma$ interval in mass resolution, where $m_{K_S^0}$ is the nominal K_S^0 mass [7]. B^0 candidates are formed by combining two K_S^0 candidates and one prompt photon candidate. The energy difference $\Delta E \equiv E_B^{\mathrm{cms}} - E_{\mathrm{beam}}^{\mathrm{cms}}$ and the beam-energy-constrained mass $M_{\mathrm{bc}} \equiv \sqrt{(E_{\mathrm{beam}}^{\mathrm{cms}})^2 - |\vec{p}_B^{\,\mathrm{cms}}|^2 c^2}/c^2$, where $E_{\mathrm{beam}}^{\mathrm{cms}}$ is the beam energy, and E_B^{cms} and $\vec{p}_B^{\,\mathrm{cms}}$ are the energy and momentum of the reconstructed B^0, respectively, are used to identify B^0 candidates. The candidates satisfying the requirements $5.20\ \mathrm{GeV}/c^2 < M_{\mathrm{bc}} < 5.29\ \mathrm{GeV}/c^2$ and $|\Delta E| < 0.5\ \mathrm{GeV}$ are retained for further analysis. We find that 6% of the events have more than one B^0 candidate. In case of multiple candidates, we choose the one with the smallest χ^2, as defined by $\chi^2 = \sum_{i=1}^{2}[(m_{K_S^0} - M_i(\pi^+\pi^-))/\sigma_{\pi\pi}]^2$, where $\sigma_{\pi\pi}$ is the mass resolution for the reconstructed K_S^0.

The dominant background arises from $e^+e^- \to q\bar{q}(q = u, d, s, c)$ continuum events. We use another NN with four input variables calculated in the CMS to suppress this background [20]: the cosine of the polar angle ($\cos\theta_B$) of the B^0 candidate flight direction; the cosine of the angle ($\cos\theta_T$) between the thrust axis of the B^0 candidate and that of the rest of the event; a flavor-tagging quality parameter of the accompanying B meson [21]; and a likelihood ratio obtained from the modified Fox-Wolfram moments [22]. The NN outputs for the signal and continuum MC events peak at $+1$ and -1, respectively. A figure-of-merit (FOM) is calculated as [23]:

$$\mathrm{FOM} = \frac{\epsilon_S(t)}{a/2 + \sqrt{N_{\mathrm{bkg}}(t)}}, \qquad (1)$$

where t is the NN output; $\epsilon_S(t)$ is the signal efficiency as a function of t determined by using the signal MC sample; N_{bkg} is the number of background events for a high t selection and a is taken to be 3 for a 3σ significance due to the low signal-to-background ratio, as suggested in Ref. [23]. The FOM is maximized for the $t > 0.93$ region which rejects 99% of the continuum MC events and retains 37% of the signal MC events. Since we expect only a few signal events and relatively large backgrounds, we further suppress the continuum background by using the helicity angle, θ_H, which is the angle between the direction opposite to the B^0 candidate and that of the K_S^0 momentum in the rest frame of the $K_S^0 K_S^0$ system. To maximize the FOM, we require $0.24 < |\cos\theta_H| < 0.86$ which removes 60% of the background while retaining 86% of the signal.

We use a Crystal Ball line shape [24] and a first-order polynomial for the signal and contributions from misreconstructed events, respectively. The signal region is defined as $-0.16\,\mathrm{GeV} < \Delta E < 0.09\,\mathrm{GeV}$ and $5.272\ \mathrm{GeV}/c^2 < M_{\mathrm{bc}} < 5.290\ \mathrm{GeV}/c^2$, corresponding to $\pm 3\sigma$ windows. In signal MC samples, about 99% of the reconstructed B^0 candidates in the signal region correctly match a true B^0.

From MC, we estimate that 2.2 ± 0.6 background events from continuum processes contribute to the signal region. In addition to the continuum, various $B\bar{B}$ background sources are also studied. Both neutral and charged $B\bar{B}$ MC samples corresponding to an integrated luminosity six times larger than that of the full data sample are used. We expect 0.3 ± 0.2 events from generic $B\bar{B}$ decays in the signal region. The decay $B^0 \to D^0(\to K_S^0\pi^0)K^0$, with a branching fraction of 5.2×10^{-5} [7], is treated separately from the generic $B\bar{B}$ because its ΔE and M_{bc} distributions are different from those of generic $B\bar{B}$ events. We estimate a contribution of about 0.1 background events from this decay.

A dedicated MC sample consisting of rare B decays was produced. Various decays with branching fractions smaller than $\mathcal{O}(10^{-4})$ are included and their total branching fraction is $\mathcal{O}(10^{-3})$. Rare B decays having one or two K_S^0 with γ in the final state can peak in the M_{bc} distribution. The backgrounds from the charged B meson pairs do not show any peaking behavior in the $\Delta E - M_{\mathrm{bc}}$ signal region. On the other hand, the background from the neutral B meson pairs peaks in the signal region and the largest contribution (34%) to the peak comes from $B^0 \to X_{d\bar{d}}\gamma$. Here, $X_{d\bar{d}}$ is a meson whose flavor wave function includes a $d\bar{d}$ pair, and all $b \to d\gamma$ processes except $B^0 \to \rho^0\gamma$ and $B \to \omega\gamma$ are included. We regard this as signal because the quark level transition and the final state are the same as for the signal. When we treat this decay mode as signal by using MC information, the peaking background is removed. Neutral and charged rare B backgrounds are estimated to be 1.0 ± 0.1 and 0.9 ± 0.1 events in the signal region, respectively.

Four additional rare decay modes which are not included in the rare B MC samples, with the following branching fractions, are considered: $\mathcal{B}(B^0 \to K_S^0 K_S^0 \pi^0) < 9 \times 10^{-7}$ [25]; $\mathcal{B}(B^0 \to K_S^0 K_S^0 \eta) < 1.0 \times 10^{-6}$; $\mathcal{B}(B^0 \to K_S^0 \pi^+\pi^-\gamma) = 1.99 \times 10^{-5}$ [26]; $\mathcal{B}(B^0 \to \pi^+\pi^-\pi^+\pi^-\pi^0) < 9.1 \times 10^{-3}$ [7]. The first two decay modes occur via a $b \to s$ quark transition and become background when π^0 or η are replaced by a photon. $B^0 \to K_S^0\pi^+\pi^-\gamma$ decays occur through a $b \to s\gamma$ quark transition and can be misidentified as the signal. $B^0 \to \pi^+\pi^-\pi^+\pi^-\pi^0$ decays occur at the tree level via a $b \to u$ transition and can be misidentified as the signal when the π^0 is replaced by a photon. We estimate that the background contribution from these four decay modes is negligible.

We estimate the total number of background events in the signal region to be 4.5 ± 0.7 via the counting method. To estimate the background events in the signal region using an extended unbinned maximum-likelihood fitting method, we fit the M_{bc} distribution satisfying -0.16 GeV $< \Delta E <$ 0.09 GeV with an ARGUS function [27] and a Crystal Ball line shape for the continuum and peaking backgrounds, respectively. The fitting parameters of the Crystal Ball line shape are fixed to those for the signal MC. We obtain 5.6 ± 0.8 background events in the signal region. This result is consistent with that of the counting method.

The signal efficiency depends on the reconstructed K_S^0-pair mass ($M_{K_S^0 K_S^0}$) as shown in Table I and is obtained from signal MC by performing an extended unbinned maximum-likelihood fit to the M_{bc} distribution satisfying -0.16 GeV $< \Delta E <$ 0.09 GeV and $5.2\ \mathrm{GeV}/c^2 < M_{\mathrm{bc}} < 5.9\ \mathrm{GeV}/c^2$ in ten equal-size bins in $M_{K_S^0 K_S^0}$ between $1\ \mathrm{GeV}/c^2$ and $3\ \mathrm{GeV}/c^2$.

The systematic uncertainties on the number of produced $B\bar{B}$ pairs and the $\Upsilon(4S) \to B^0\bar{B}^0$ branching fraction are 1.4% and 1.2% [7], respectively. The systematic uncertainty in the photon detection efficiency is studied using radiative Bhabha events and estimated to be 2.0% [28]. Using a systematic uncertainty of 0.2% for K_S^0 reconstruction efficiency and per track uncertainty in efficiency of 0.4% [29] leads to the estimate of 1.4% for the uncertainty in the reconstruction efficiency for the two $K_S^0 \to \pi^+\pi^-$ decays. The systematic uncertainty due to the

TABLE I. Summary of the number of observed events (N_{obs}), number of estimated background events (N_{bkg}), efficiencies (ϵ_S), upper limits on the signal yield (S_{90}), and branching fraction upper limits (U.L.) at the 90% C.L. in each $M_{K_S^0 K_S^0}$ bin for the $B^0 \to K_S^0 K_S^0 \gamma$ decay.

Mass bin (GeV/c^2)	ϵ_S (%)	N_{bkg}	σ_{sys} (%)	N_{obs}	S_{90}	U.L. (10^{-7})
1.0–1.2	3.3	0.8 ± 0.3	3.2	0	1.8	0.7
1.2–1.4	3.0	0.9 ± 0.3	3.2	3	6.5	2.8
1.4–1.6	2.7	0.8 ± 0.3	3.2	1	3.6	1.7
1.6–1.8	2.5	0.3 ± 0.1	3.2	0	2.1	1.1
1.8–2.0	2.3	0.8 ± 0.3	3.2	2	5.1	2.9
2.0–2.2	2.2	0.2 ± 0.1	3.2	1	4.2	2.5
2.2–2.4	2.2	0.4 ± 0.2	3.2	1	3.9	2.4
2.4–2.6	2.2	0.2 ± 0.2	3.2	0	2.2	1.3
2.6–2.8	2.3	0.0 ± 0.0	3.2	1	4.2	2.3
2.8–3.0	2.4	0.1 ± 0.0	3.2	0	2.3	1.2

background suppression using the NN selection and π^0/η veto is 0.6% [28]. The signal efficiency depends on $M_{K_S^0 K_S^0}$ and the MC statistical uncertainty in the efficiency varies between 0.5% and 0.7% depending on $M_{K_S^0 K_S^0}$. The total systematic uncertainty is 3.2% and is summarized in Table II.

There are 9 events in the ΔE-M_{bc} signal region. The fit to the M_{bc} distribution is carried out with an extended unbinned maximum-likelihood with a Crystal Ball line shape including contributions from the peaking background for the signal and an ARGUS function for the background, respectively, as shown in Fig. 2. We obtain 3.8 ± 3.0 signal and 5.6 ± 0.8 background events in the signal region. The fitting parameters for the signal are fixed to those for the signal MC. The number of the background events in the signal region agrees well with that of the estimated background events in the signal region from MC samples.

The $|\cos\theta_H|$ distributions for events in the $\Delta E - M_{bc}$ signal region are shown in Fig. 3 for data and MC samples. The $|\cos\theta_H|$ distribution results from data are consistent with MC simulation.

The observed number of events in each $M_{K_S^0 K_S^0}$ bin is obtained by counting the events in the ΔE-M_{bc} signal region. Figure 4 shows the observed number of events

TABLE II. Systematic uncertainties in branching fractions.

Source	Uncertainty (%)
Number of $B\bar{B}$	1.4
Branching fraction of $\Upsilon(4S) \to B^0\bar{B}^0$	1.2
Photon detection efficiency	2.0
Two K_S^0 reconstruction	1.4
NN selection and π^0/η veto	0.6
MC statistics in $M_{K_S^0 K_S^0}$ bin efficiency	0.5–0.7
Total	3.2

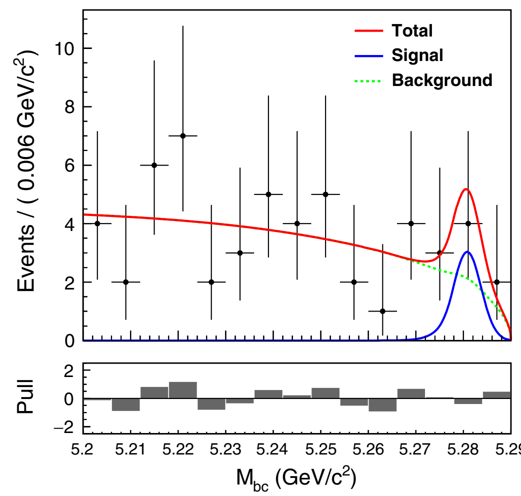

FIG. 2. Distribution of the data in the variable M_{bc}, together with the fit to contributions from background and signal events, after requiring -0.16 GeV $< \Delta E < 0.09$ GeV and $0.24 < |\cos\theta_H| < 0.86$.

(N_{obs}) in the full data sample and the estimated background events in each $M_{K_S^0 K_S^0}$ bin. No significant excess over the estimated background is observed in the data, and we derive an upper limit for the signal yield (S_{90}) at the 90% confidence level (C.L.) using the POLE program by taking into account the uncertainties associated with the signal selection efficiency, background expectation, and systematic uncertainty [30]. The branching fractions are obtained from

$$\mathcal{B}(B^0 \to K_S^0 K_S^0 \gamma) = \frac{S_{90}}{\epsilon_S \times N_{B\bar{B}}}, \quad (2)$$

where $N_{B\bar{B}}$ and ϵ_S are the number of $B\bar{B}$ pairs and signal efficiency, respectively. We obtain 90% C.L. upper limits on the partial branching fractions for the decay

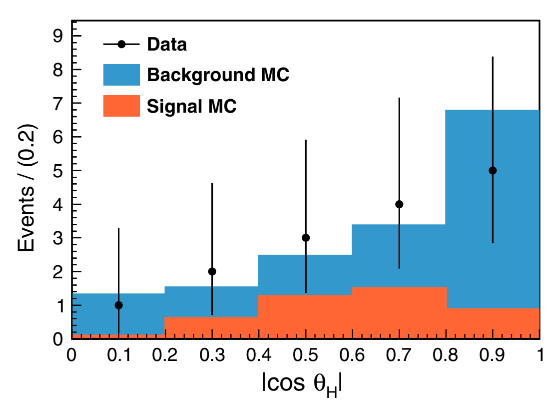

FIG. 3. The helicity angle distribution of the observed events in the signal region. The background and signal histograms are stacked.

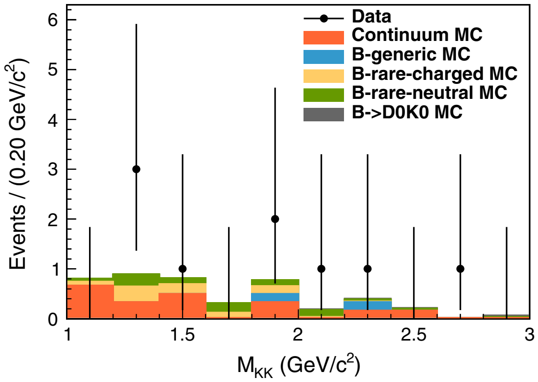

FIG. 4. The $M_{K_S^0 K_S^0}$ distribution in the signal region. The dots represent data and the stacked histograms are the estimated number of backgrounds from the MC background samples.

$B^0 \to K_S^0 K_S^0 \gamma$ in ten bins of $M_{K_S^0 K_S^0}$ for $1.0\ \mathrm{GeV}/c^2 < M_{K_S^0 K_S^0} < 3.0\ \mathrm{GeV}/c^2$, which are listed in Table I.

For the full range $1.0\ \mathrm{GeV}/c^2 < M_{K_S^0 K_S^0} < 3.0\ \mathrm{GeV}/c^2$, we use the average efficiency of all bins, $(2.5 \pm 0.4)\%$. The standard deviation of efficiencies among $M_{K_S^0 K_S^0}$ bins is assigned as a systematic uncertainty (16.0%). Adding to other systematic uncertainties listed in Table II in quadrature, the total systematic uncertainty is 16.2%. Using the POLE program with 9 observed events and expected background of 4.5 ± 0.7, we obtain the upper limit on the branching fraction for the $1.0\ \mathrm{GeV}/c^2 < M_{K_S^0 K_S^0} < 3.0\ \mathrm{GeV}/c^2$ mass range to be 5.8×10^{-7} at the 90% C.L.

We also obtain upper limits on the product branching fractions for the intermediate tensor f_2 states, $\mathcal{B}(B^0 \to f_2\gamma) \times \mathcal{B}(f_2 \to K_S^0 K_S^0)$. The signal mass regions are taken to be $1.00\ \mathrm{GeV}/c^2 < M_{K_S^0 K_S^0} < 1.44\ \mathrm{GeV}/c^2$ and $1.44\ \mathrm{GeV}/c^2 < M_{K_S^0 K_S^0} < 1.63\ \mathrm{GeV}/c^2$ for $f_2(1270)$ and $f_2'(1525)$, respectively. These mass regions contain 80% of signal events. The results are summarized in Table III.

In summary, we have reported the results from the first search for radiative B-meson decays to the $K_S^0 K_S^0 \gamma$ final state using a data sample of $772 \times 10^6 B\bar{B}$ pairs. No significant signal is observed for the full data sample. The signal efficiency depends on $M_{K_S^0 K_S^0}$ and we obtain upper limits at the 90% C.L. on the partial branching fractions for the decay $B^0 \to K_S^0 K_S^0 \gamma$ in ten bins of $M_{K_S^0 K_S^0}$ for $1.0\ \mathrm{GeV}/c^2 < M_{K_S^0 K_S^0} < 3.0\ \mathrm{GeV}/c^2$ to be $[0.7\text{–}2.9] \times 10^{-7}$. We also obtain an upper limit on its branching fraction as 5.8×10^{-7} at the 90% C.L. for the $1.0\ \mathrm{GeV}/c^2 < M_{K_S^0 K_S^0} < 3.0\ \mathrm{GeV}/c^2$ mass range. The upper limits at the 90% C.L. on the products of the branching fractions $\mathcal{B}(B^0 \to f_2\gamma) \times \mathcal{B}(f_2(1270) \to K_S^0 K_S^0)$ and $\mathcal{B}(B^0 \to f_2'\gamma) \times \mathcal{B}(f_2'(1525) \to K_S^0 K_S^0)$ are obtained to be 3.1×10^{-7} and 2.1×10^{-7}, respectively.

We thank the KEKB group for the excellent operation of the accelerator; the KEK cryogenics group for the efficient operation of the solenoid; and the KEK computer group, and the Pacific Northwest National Laboratory (PNNL) Environmental Molecular Sciences Laboratory (EMSL) computing group for strong computing support; and the National Institute of Informatics, and Science Information NETwork 5 (SINET5) for valuable network support. We acknowledge support from the Ministry of Education, Culture, Sports, Science, and Technology (MEXT) of Japan, the Japan Society for the Promotion of Science (JSPS), and the Tau-Lepton Physics Research Center of Nagoya University; the Australian Research Council including Grants No. DP180102629, No. DP170102389, No. DP170102204, No. DP150103061, No. FT130100303; Austrian Federal Ministry of Education, Science and Research (FWF) and FWF Austrian Science Fund No. P 31361-N36; the National Natural Science Foundation of China under Contracts No. 11435013, No. 11475187, No. 11521505, No. 11575017, No. 11675166, No. 11705209; Key Research Program of Frontier Sciences, Chinese Academy of Sciences (CAS), Grant No. QYZDJ-SSW-SLH011; the CAS Center for Excellence in Particle Physics (CCEPP); the Shanghai Science and Technology Committee (STCSM) under Grant No. 19ZR1403000; the Ministry of Education, Youth and Sports of the Czech Republic under Contract No. LTT17020; Horizon 2020 ERC Advanced Grant No. 884719 and ERC Starting Grant No. 947006 "InterLeptons" (European Union); the Carl Zeiss Foundation, the Deutsche Forschungs gemeinschaft, the Excellence Cluster Universe, and the VolkswagenStiftung; the Department of Atomic Energy (Project Identification No. RTI 4002) and the Department of Science and Technology of India; the Istituto Nazionale

TABLE III. Summary of the number of observed events (N_{obs}), number of estimated background events (N_{bkg}), efficiencies (ϵ_S), upper limits on the signal yield (S_{90}), and product branching fraction upper limits (U.L.) at the 90% C.L. for the $B^0 \to f_2\gamma$ and $f_2 \to K_S^0 K_S^0$ decays.

Branching fraction product	$\epsilon_S(\%)$	N_{bkg}	$\sigma_{\mathrm{sys}}(\%)$	N_{obs}	S_{90}	U.L.(10^{-7})
$B^0 \to f_2(1270)(\to K_S^0 K_S^0)\gamma$	2.3	1.8 ± 0.4	3.1	3	5.7	3.1
$B^0 \to f_2'(1525)(\to K_S^0 K_S^0)\gamma$	2.2	0.8 ± 0.3	3.1	1	3.6	2.1

di Fisica Nucleare of Italy; National Research Foundation (NRF) of Korea Grants No. 2016R1D1A1B01010135, No. 2016R1D1A1B02012900, No. 2018R1A2B3003643, No. 2018R1A6A1A06024970, No. 2019K1A3A7A09033840, No. 2019K1A3A7A09034974, No. 2019R1I1A3A01058933, No. 2021R1A6A1A03043957, No. 2021R1F1A1060423, No. 2021R1F1A1064008; Radiation Science Research Institute, Foreign Large-size Research Facility Application Supporting project, the Global Science Experimental Data Hub Center of the Korea Institute of Science and Technology Information and KREONET/GLORIAD; the Polish Ministry of Science and Higher Education and the National Science Center; the Ministry of Science and Higher Education of the Russian Federation, Agreement 14.W03.31.0026, and the HSE University Basic Research Program, Moscow; University of Tabuk research Grants No. S-1440-0321, No. S-0256-1438, and No. S-0280-1439 (Saudi Arabia); the Slovenian Research Agency Grants No. J1-9124 and No. P1-0135; Ikerbasque, Basque Foundation for Science, Spain; the Swiss National Science Foundation; the Ministry of Education and the Ministry of Science and Technology of Taiwan; and the United States Department of Energy and the National Science Foundation.

[1] J. Ellis, M. K. Gaillard, D. V. Nanopoulos, and S. Rudaz, Nucl. Phys. **B131**, 285 (1977); **B132**, 541(E) (1978); Tobias Hurth and Mikihiko Nakao, Annu. Rev. Nucl. Part. Sci. **60**, 645 (2010).

[2] A. J. Buras, Lect. Notes Phys. **558**, 65 (2000).

[3] T. Hurth, E. Lunghi, and W. Porod, Nucl. Phys. **B704**, 56 (2005).

[4] G. C. Branco, P. M. Ferreira, L. Lavoura, M. N. Rebelo, M. Sher, and J. P. Silva, Phys. Rep. **516**, 1 (2012).

[5] M. Kobayashi and T. Maskawa, Prog. Theor. Phys. **49**, 652 (1973); N. Cabibbo, Phys. Rev. Lett. **10**, 531 (1963).

[6] M. Misiak *et al.*, Phys. Rev. Lett. **114**, 221801 (2015); M. Misiak, A. Rehman, and M. Steinhauser, J. High Energy Phys. 06 (2020) 175.

[7] P. A. Zyla *et al.* (Particle Data Group), Prog. Theor. Exp. Phys. **2020**, 083C01 (2020); S. Chen *et al.* (CLEO Collaboration), Phys. Rev. Lett. **87**, 251807 (2001); A. Limosani *et al.* (Belle Collaboration), Phys. Rev. Lett. **103**, 241801 (2009); T. Saito *et al.* (Belle Collaboration), Phys. Rev. D **91**, 052004 (2015); B. Aubert *et al.* (*BABAR* Collaboration), Phys. Rev. D **77**, 051103(R) (2008); J. P. Lees *et al.* (*BABAR* Collaboration), Phys. Rev. Lett. **109**, 191801 (2012); J. P. Lees *et al.* (*BABAR* Collaboration), Phys. Rev. D **86**, 052012 (2012); P. del Amo Sanchez *et al.* (*BABAR* Collaboration), Phys. Rev. D **82**, 051101(R) (2010).

[8] R. Aaij *et al.* (LHCb Collaboration), Nucl. Phys. **B867**, 1 (2013); B. Aubert *et al.* (*BABAR* Collaboration), Phys. Rev. Lett. **103**, 211802 (2009); M. Nakao *et al.* (Belle Collaboration), Phys. Rev. D **69**, 112001 (2004); T. Horiguchi *et al.* (Belle Collaboration), Phys. Rev. Lett. **119**, 191802 (2017); T. E. Coan *et al.* (CLEO Collaboration), Phys. Rev. Lett. **84**, 5283 (2000).

[9] H. Yang *et al.* (Belle Collaboration), Phys. Rev. Lett. **94**, 111802 (2005).

[10] H. Sahoo *et al.* (Belle Collaboration), Phys. Rev. D **84**, 071101(R) (2011); B. Aubert *et al.* (*BABAR* Collaboration), Phys. Rev. D **75**, 051102 (2007); A. Drutskoy *et al.* (Belle Collaboration), Phys. Rev. Lett. **92**, 051801 (2004).

[11] R. Wedd *et al.* (Belle Collaboration), Phys. Rev. D **81**, 111104(R) (2010).

[12] S. Nishida *et al.* (Belle Collaboration), Phys. Lett. B **610**, 23 (2005);

[13] N. Taniguchi *et al.* (Belle Collaboration), Phys. Rev. Lett. **101**, 111801 (2008); B. Aubert *et al.* (*BABAR* Collaboration), Phys. Rev. Lett. **98**, 151802 (2007); D. Mohapatra *et al.* (Belle Collaboration), Phys. Rev. Lett. **96**, 221601 (2006).

[14] S. Kurokawa and E. Kikutani, Nucl. Instrum. Methods Phys. Res., Sect. A **499**, 1 (2003), and other papers included in this volume; T. Abe *et al.*, Prog. Theor. Exp. Phys. **483**, 03A001 (2013), and following articles up to 03A011.

[15] A. Abashian *et al.* (Belle Collaboration), Nucl. Instrum. Methods Phys. Res., Sect. A **479**, 117 (2002); Also, see the detector section in J. Brodzicka *et al.*, Prog. Theor. Exp. Phys. **2012**, 04D001 (2012).

[16] D. J. Lange, Nucl. Instrum. Methods Phys. Res., Sect. A **462**, 152 (2001).

[17] R. Brun *et al.*, CERN Report No. CERN DD/EE/84-1, 1984.

[18] P. Koppenburg *et al.* (Belle Collaboration), Phys. Rev. Lett. **93**, 061803 (2004).

[19] H. Nakano, Ph.D. thesis, Tohoku University, 2014; H. Nakano *et al.* (Belle Collaboration), Phys. Rev. D **97**, 092003 (2018).

[20] M. Feindt and U. Kerzel, Nucl. Instrum. Methods Phys. Res., Sect. A **559**, 190 (2006).

[21] H. Kakuno *et al.* (Belle Collaboration), Nucl. Instrum. Methods Phys. Res., Sect. A **533**, 516 (2004).

[22] R. O. Duda, P. E. Hart, and D. G. Stork, *Pattern Classification*, 2nd ed. (John Wiley & Sons, New York, 2001); G. C. Fox and S. Wolfram, Phys. Rev. Lett. **41**, 1581 (1978); S. H. Lee *et al.* (Belle Collaboration), Phys. Rev. Lett. **91**, 261801 (2003).

[23] G. Punzi, in *Proceedings of the Statistical Problems in Particle Physics, Astrophysics and Cosmology, Conference, PHYSTAT 2003, Stanford, USA, eConf C030908, MODT002* (SLAC, 2003), https://www.slac.stanford.edu/econf/C030908/papers/MODT002.pdf.

[24] T. Skwarnicki, Ph.D. thesis, Institute for Nuclear Physics, Krakow, DESY Internal Report No. DESY F31-86-02, 1986.

[25] B. Aubert *et al.* (*BABAR* Collaboration), Phys. Rev. D **80**, 011101(R) (2009).
[26] H. Yang *et al.* (Belle Collaboration), Phys. Rev. Lett. **94**, 111802 (2005); P. del Amo Sanchez *et al.* (*BABAR* Collaboration), Phys. Rev. D **93**, 052013 (2016).
[27] H. Albrecht *et al.* (ARGUS Collaboration), Phys. Lett. B **229**, 304 (1989).
[28] T. Horiguchi *et al.* (Belle Collaboration), Phys. Rev. Lett. **119**, 191802 (2017).
[29] S. Jia *et al.* (Belle Collaboration), Phys. Rev. D **100**, 032006 (2019).
[30] J. Conrad, O. Botner, A. Hallgren, and C. Pérez de los Heros, Phys. Rev. D **67**, 012002 (2003); G. J. Feldman and R. D. Cousins, Phys. Rev. D **57**, 3873 (1998).